JOURNAL OF SOLID STATE CHEMISTRY 118, 117–124 (1995)

Thermochemical Stability, Electrical Conductivity, and Seebeck Coefficient of Sr-Doped $LaCo_{0.2}Fe_{0.8}O_{3-\delta}$

L-W. Tai,[1] M. M. Nasrallah,[2] and H. U. Anderson

Ceramic Engineering Department, University of Missouri–Rolla, Rolla, Missouri 65401

Received September 1, 1994; in revised form January 30, 1995; accepted February 2, 1995

Phase stability, oxygen content, electrical conductivity, and Seebeck coefficient of $La_{1-x}Sr_xCo_{0.2}Fe_{0.8}O_{3-\delta}$ (x = 0, 0.2, 0.4) were studied as a function of temperature and oxygen activity. The thermochemical properties of these compositions under a reducing atmosphere appear to follow the boundaries set between the two end members, $LaFeO_3$ and $LaCoO_3$, but the electrical properties are closer to those of $LaFeO_3$. The Sr content ($x \leq 0.4$) does not seem to have a significant effect on the high-temperature phase stability. Dissociation of these compositions under a reducing atmosphere occurred gradually by the formation of transient compounds. The major transient compounds formed during dissociation could be represented by a general formula of (La,Sr)(Fe,Co)O_4. Upon further reduction, these oxides dissociated to La_2O_3, SrO, Co, and Fe. © 1995 Academic Press, Inc.

1. INTRODUCTION

Perovskite-type oxides (ABO_3), with rare earth elements on the A sites and transition metals on the B sites, are well known for their refractory properties, catalytic activities, and wide range of electrical properties. Among them, the acceptor-doped $A^{3+}B^{3+}O_3$ (A = La, Y; B = Mn, Fe, Co, Ni) compositions have been evaluated as the cathode in solid oxide fuel cells (SOFC) (1). In a separate study (2), it was found that compositions of $La_{1-x}Sr_xCo_{0.2}Fe_{0.8}O_{3-\delta}$ (LSCF, x = 0–0.4) possess higher electrical conductivity than that of Sr-doped $LaMnO_3$, which is currently being used as the cathode for SOFCs. The LSCF compositions are also potential candidates for oxygen-separation membranes, due to their apparent mixed ionic–electronic conductivity at intermediate temperatures (600–800°C).

Understanding the oxygen nonstoichiometry and thermochemical stability of the LSCF, under SOFC or oxygen-separation membrane operating conditions, is as important as understanding their electrical conductivity. Electrical conductivity, Seebeck coefficient, and the defect structure of $La_{1-x}Sr_xFeO_3$ (x = 0–0.6) and $La_{1-x}Sr_xCoO_3$ (x = 0–0.7) have been extensively studied (3–7). The phase stability of $LaFeO_3$ and $LaCoO_3$ under reducing atmospheres has been studied by Nakamura *et al.* (8). However, the high-temperature phase stability and electrical properties of Sr-doped $LaCo_{1-y}Fe_yO_3$ as function of oxygen activity have not been established. The present investigation examines the phase stability, oxygen nonstoichiometry, electrical conductivity, and Seebeck coefficient of $La_{1-x}Sr_xCo_{0.2}Fe_{0.8}O_3$ as function of temperature, oxygen activity, and Sr content.

2. EXPERIMENTAL PROCEDURE

Oxide powders of $La_{1-x}Sr_xCo_{0.2}Fe_{0.8}O_{3-\delta}$ (x = 0, 0.2, 0.4) were prepared by the liquid-mix process (2). The calcined powders were single-phase perovskite as determined by X-ray diffraction, using a Scintag XRD-2000 diffractometer. Before each thermogravimetric (TG) run, the powder sample was annealed at 1250°C for 24 hr to ensure the removal of volatile matter. Annealing also reduced the apparent volume of powders, thus allowing the placement of more sample (≥25 g) in the cylindrical alumina crucible (volume of 50 cm^3) for the TG measurement. A mass-flow controller that set the composition and flow of gas mixtures consisting of either O_2/N_2 or CO_2/forming gas (10% H_2 in N_2) was used to establish the desired oxygen activity. The gas flow system was precalibrated and monitored with an oxygen sensor. The real-time weight change during a TG run was monitored and displayed graphically with an IBM PC. A detailed description of the thermogravimetric apparatus has been reported elsewhere (9).

The TG runs were initiated after equilibrating the LSCF sample under pure oxygen at 1200°C. When the sample weight remained unchanged for 24 hr, the oxide was considered to be in equilibrium with the given oxygen activity and the sample weight was recorded. The oxygen activity was then reduced by steps of about one order of magnitude to 10^{-19}. Finally, to confirm revers-

[1] Current address: General Motors Research & Development Center, Electrical & Electronics Department, Warren, MI 48090-9055.

[2] On leave from Faculty of Engineering, Cairo University, Egypt.

0022-4596/95 $12.00

ibility, reoxidation of the fully reduced sample to its original state was achieved by introducing oxygen. This is required since the presence of any volatile species other than oxygen will cause irreversible weight loss and makes the analysis of oxygen content impossible.

Phase stability and the dissociated products of LSCF compositions under reducing atmospheres were studied by using quench experiments. Powder samples (5–7 g) were placed in an alumina boat and equilibrated at a given temperature and oxygen activity for 2 to 4 weeks in a muffle furnace. The samples were then quenched by pulling the crucible to the cool zone of the furnace (≈50°C) under the same atmosphere in about 10 sec to preserve the high-temperature phase(s). The as-quenched powder samples were immediately weighted to determine weight loss and examined by XRD, using a SCINTAG XRD-2000 diffractometer with a Cu target and Ni filter. The presence of Co metal in the reduced samples was detected by a GE XRD-5 diffractometer with a Co target.

Electrical conductivity and Seebeck coefficients of sintered samples were measured using a computer-driven apparatus capable of carrying out two-point, four-wire Kelvin technique electrical conductivity measurements and thermoelectric power measurements simultaneously on the same sample (10). To verify the reliability of the measured dc conductivity, a four-probe ac measurement was also performed at a frequency of 100 Hz on selected samples. The atmosphere control was provided by the same type of gas flow system used in the TG and annealing–quenching experiments. The sample resistance was monitored at 30-min. intervals until equilibration was attained at a given oxygen activity.

3. RESULTS AND DISCUSSION

The weight losses observed for various $La_{1-x}Sr_x Co_{0.2}Fe_{0.8}O_{3-\delta}$ compositions upon heating under oxygen are shown in Fig. 1. As can be seen, for the undoped sample, weight change is not apparent at 1100°C. The maximum weight loss (≈1%, at 1200°C) occurred for the composition with Sr = 0.4. These weight changes were found to be reversible and dependent on the ambient oxygen activity. It was therefore concluded that this weight loss was due to oxygen evolution from the oxide sample. The thermogravimetric behavior observed in Fig. 1 indicates that the acceptor dopant of Sr induced the formation of more oxygen vacancies at lower temperatures.

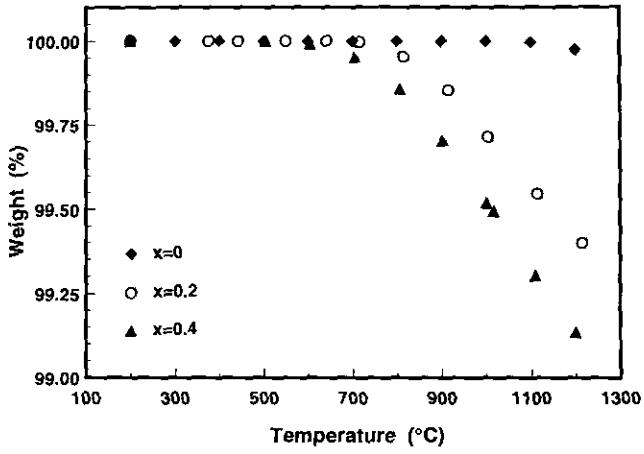

FIG. 1. Relative weight change of $La_{1-x}Sr_xCo_{0.2}Fe_{0.8}O_3$ as a function of Sr content (moles) and temperature, under oxygen.

The room-temperature oxygen content for each composition was determined using weight-loss data from the TG and quenching experiments. A reference point was established by fully reducing LSCF into its components of La_2O_3, SrO, Co, and Fe at 1200°C. The dissociated sample was then quenched (under a reducing atmosphere) and the final weight was quickly measured. It was assumed that the cation contents did not change after being dissociated and that La_2O_3 and SrO still remained stoichiometric under the most reducing condition applied (oxygen activity of 10^{-19}). Using this reference point and the weight loss curves in Fig. 1, the compositions at both elevated temperature and room temperature were calculated. Table 1 lists the oxygen content for compositions with Sr = 0, 0.2, and 0.4 at the specified temperature and ambient atmosphere.

Unlike $LaFeO_3$, which was reported to be oxygen deficient in air (3, 11), the oxygen content in $LaCo_{0.2}Fe_{0.8}O_{3-\delta}$ was found to be nearly stoichiometric at temperatures up

TABLE 1
Oxygen Content (moles) of LSCF Compositions under Various Conditions

Oxygen content ($3-\delta$)	Room temperature in air	1000°C under oxygen	1200°C under oxygen
$LaCo_{0.2}Fe_{0.8}O_{3-\delta}$	3.005 ± 0.010	3.005 ± 0.015	3.003 ± 0.010
$La_{0.8}Sr_{0.2}Co_{0.2}Fe_{0.8}O_{3-\delta}$	2.999 ± 0.003	2.992 ± 0.005	2.972 ± 0.003
$La_{0.6}Sr_{0.4}Co_{0.2}Fe_{0.8}O_{3-\delta}$	2.948 ± 0.009	2.908 ± 0.005	2.849 ± 0.006

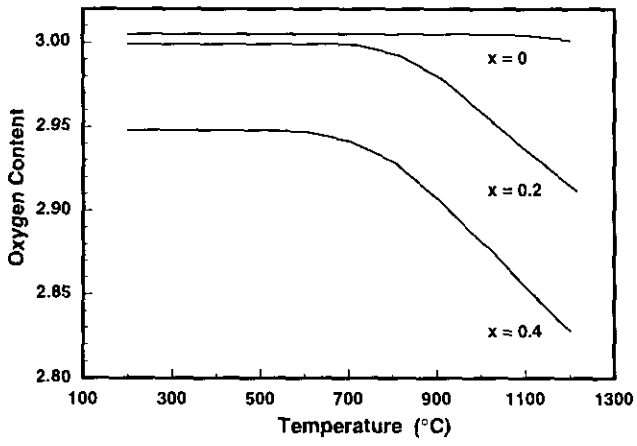

FIG. 2. Oxygen content (moles) of $La_{1-x}Sr_xCo_{0.2}Fe_{0.8}O_{3-\delta}$ compositions calculated from TG data in Fig. 1, as a function of temperature and Sr content (moles), under oxygen.

to 1200°C. As shown by these data in Table 1, the addition of Sr resulted in oxygen deficiency, which increased with Sr content. Figure 2 shows the oxygen content for each composition calculated as a function of temperature.

The weight loss of LSCF compositions as a function of oxygen activity was measured at 1200°C, and the calculated oxygen content is shown in Fig. 3. As can be seen in Fig. 3, all three compositions show a significant decrease in oxygen content at an oxygen activity of 10^{-13}, with a minimum in the region of 10^{-15} to 10^{-16}. No further weight change was detected for oxygen activity $\leq 10^{-16}$. The XRD results (discussed later) show that a series of distinct defect reactions and reduction processes occur as the oxygen activity decreases, and the complete dissociation to binary oxides and metals happens at an oxygen activity $\leq 10^{-16}$.

In the oxide of $LaBO_3$, a condition of "electronic stoichiometry" is achieved when all the transition B ions are in the trivalent state (11). This type of behavior was typically seen in the Sr-doped $LaFeO_3$ (4). Under this condition, an oxygen-activity-independent region would be observed with an oxygen content that is related to the acceptor concentration, which for LSCF would be $3 - x/2$. For the LSCF samples investigated, the oxygen content at which the electronic stoichiometry would have been reached should be 2.9 and 2.8 for the compositions with $x = 0.2$ and 0.4, respectively. As can be seen in Fig. 3, the LSCF compositions do not show the expected oxygen-activity-independent region at these particular oxygen contents. However, as will be shown later, electrical conductivity and Seebeck coefficient did indicate that an electronic stoichiometry was achieved in these compositions when $10^{-5} \leq$ oxygen activity $\leq 10^{-3}$ at 1200°C. This may be due to the presence of more than one type of B-site cation and the existence of various valence states, thus complicating the reduction process.

The high-temperature phase stability of $LaFeO_3$ and $LaCoO_3$ has been studied by Nakamura *et al.* (8). At 1200°C, undoped $LaFeO_3$ was stable in the perovskite phase above a critical oxygen activity of $10^{-13.5}$. The dissociation of $LaFeO_3$ (into La_2O_3 and Fe) occurred in one simple step. On the other hand, $LaCoO_3$ was much less stable under a reducing atmosphere, it formed several intermediate phases before La_2O_3 and Co finally formed (see Fig. 4 for the phase-stability diagram at 1000°C). Iron ions are very stable in the +3 valence state, whereas Co ions tend to stabilize in the +2 valence state, thus influencing the stability range of the A^{3+} B^{3+} O_3 perovskite structure.

Figure 5 shows the XRD patterns of quenched $La_{0.6}Sr_{0.4}Co_{0.2}Fe_{0.8}O_3$ powders after equilibration at vari-

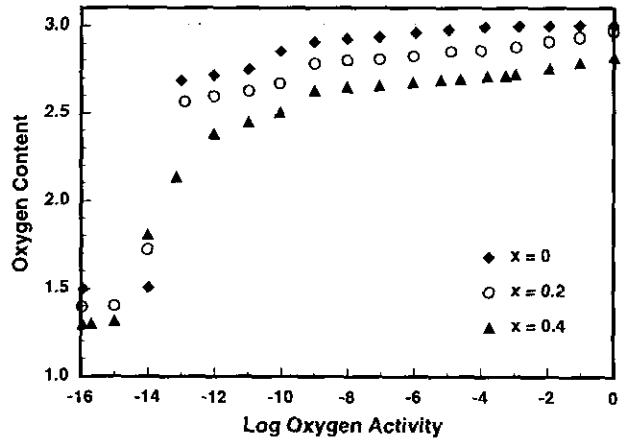

FIG. 3. Oxygen content (moles) of $La_{1-x}Sr_xCo_{0.2}Fe_{0.8}O_{3-\delta}$ as a function of oxygen activity and Sr content (moles) at 1200°C.

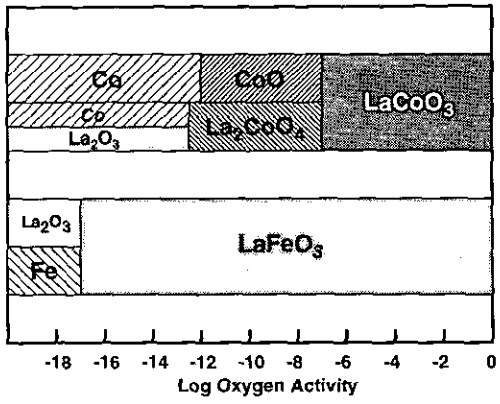

FIG. 4. The phase dissociation of $LaFeO_3$ and $LaCoO_3$ at 1000°C reported by Nakamura *et al.* (8).

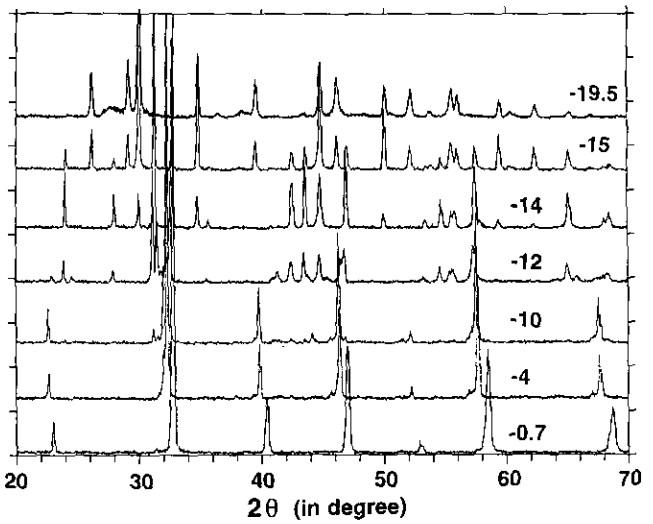

FIG. 5. XRD patterns for $La_{0.6}Sr_{0.4}Co_{0.2}Fe_{0.8}O_3$ annealed at 1200°C and quenched at given oxygen activities.

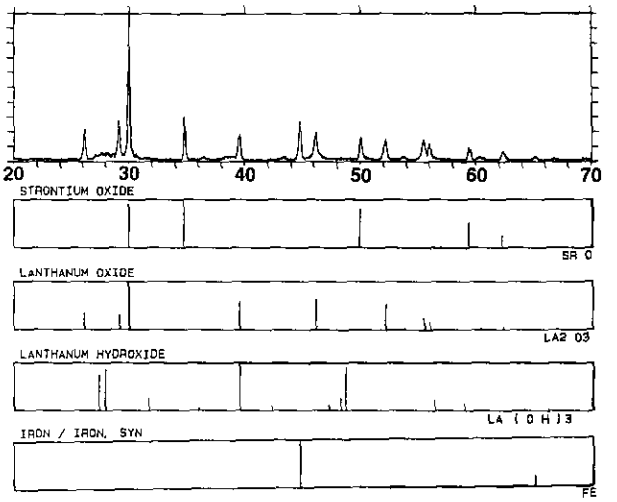

FIG. 7. XRD patterns for $La_{0.6}Sr_{0.4}Co_{0.2}Fe_{0.8}O_3$ annealed at 1200°C and quenched at an oxygen activity of $10^{-19.5}$ (in forming gas).

ous oxygen activities at a temperature of 1200°C. The LSCF perovskite phase remains the dominating phase for an oxygen activity $\geq 10^{-10}$. However, below this oxygen activity, new phase(s) start to form, as indicated by the new weak peaks that appeared in the XRD patterns. The nature of these transient phases and their formation/elimination will be discussed later. The perovskite phase completely disappeared at an oxygen activity of 10^{-14}, with the simultaneous formation of new phases identified as SrO and Fe (see Fig. 6). Cobalt was detected in all samples heated at 1200°C in oxygen activity $<10^{-10}$, but does not appear in the patterns shown in Figs. 6 and 7

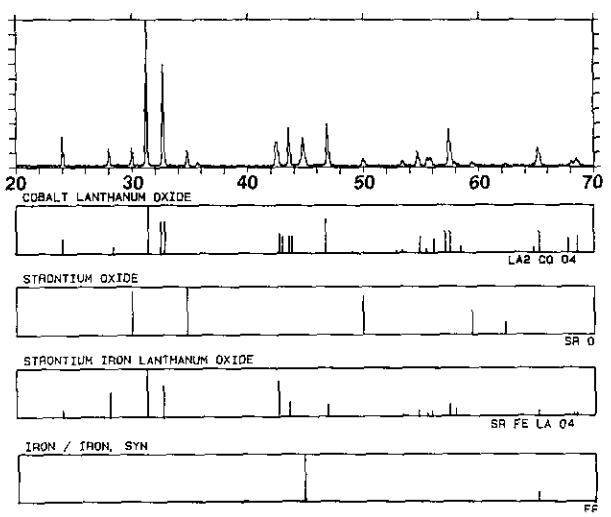

FIG. 6. XRD patterns for $La_{0.6}Sr_{0.4}Co_{0.2}Fe_{0.8}O_3$ annealed at 1200°C and quenched at an oxygen activity of 10^{-14}.

because those XRD patterns resulted from using $CuK\alpha_1$ radiation, which could not detect Co. In contrast to the findings of Nakamura *et al.* (8), who reported that at oxygen activity $10^{-13.5}$ and 1200°C, $LaFeO_3$ dissociated to La_2O_3 and Fe in a single step, the results from XRD analyses indicate that Sr-doped LSCF decomposed into some intermediate compounds of $LaSrFeO_4$ which were stable against reduction until the oxygen activity became $\leq 10^{-15}$ at 1200°C, when La_2O_3 was evolved. The XRD pattern of LSCF annealed and quenched at an oxygen activity of 10^{-14} at 1200°C is shown in Fig. 6 along with JCPDS standard peaks for SrO, Fe, $LaSrFeO_4$, and La_2CoO_4. The XRD patterns of $LaSrFeO_4$ and La_2CoO_4 appear to be similar and match that of quenched LSCF. Both $LaSrFeO_4$ and La_2CoO_4 possess K_2NiF_4-type structure (with a certain degree of distortion) (12, 13). It seems that they are relatively stable under the reducing atmosphere, when Fe and Co ions exist in trivalent and divalent states, respectively. It is likely that under these conditions LCSF forms either a solid solution or a mechanical mixture, represented by (La,Sr)(Fe,Co)O_4, in which the ratios of La/Sr and Fe/Co changed with oxygen activity and temperature.

XRD analyses showed that (at 1200°C) both undoped and Sr-doped $LaCo_{0.2}Fe_{0.8}O_3$ fully dissociated into La_2O_3, SrO, plus Co and Fe for oxygen activity $\leq 10^{-16}$. This is illustrated by Fig. 7, which is from a quenched powder of $La_{0.6}Sr_{0.4}Co_{0.2}Fe_{0.8}O_3$ that had been heated for 10 days at oxygen activity of $10^{-19.5}$ at 1200°C. The observed $La(OH)_3$ is due to hydrolysis of the freshly reduced La_2O_3 by the moisture in air. Figure 8 shows the phase development when $La_{0.6}Sr_{0.4}Co_{0.2}Fe_{0.8}O_3$ was heated to 1200°C as function of oxygen activity. The general expression of

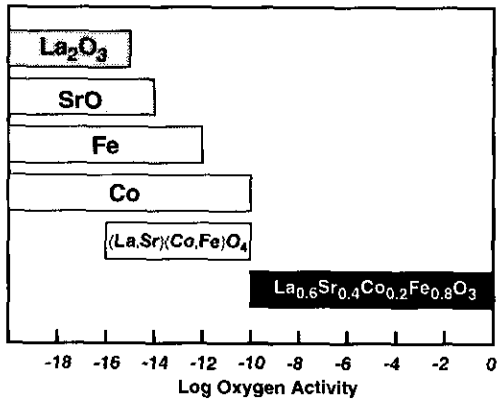

FIG. 8. The equilibrium phases(s) of $La_{0.6}Sr_{0.4}Co_{0.2}Fe_{0.8}O_3$ at 1200°C as a function of oxygen activity (from XRD analyses).

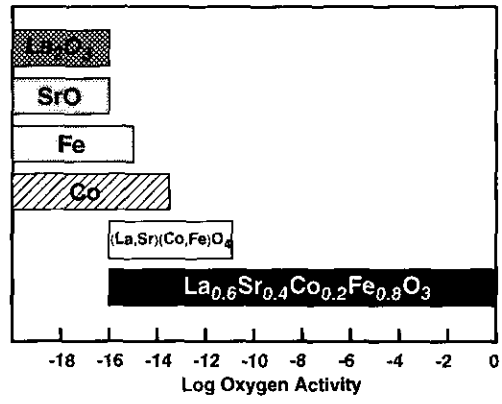

FIG. 10. The equilibrium phases(s) of $La_{0.6}Sr_{0.4}Co_{0.2}Fe_{0.8}O_3$ at 1000°C as a function of oxygen activity (from XRD analyses).

$(La,Sr)(Fe,Co)O_4$ was used to represent the transient oxide(s) observed between $10^{-16} \leq$ oxygen activity $\leq 10^{-10}$. However, it is suspected that the formation of $(La,Sr)(Fe,Co)O_4$ may have begun at an oxygen activity $\geq 10^{-10}$, which is reflected in the electrical conductivity and Seebeck data to be discussed later.

XRD patterns and phase analyses on $La_{0.6}Sr_{0.4}Co_{0.2}Fe_{0.8}O_{3-\delta}$, equilibrated at 1000°C as function of oxygen activity, are shown in Figs. 9 and 10, respectively. As expected, the perovskite phase was stable over a wider oxygen activity range than at 1200°C, and the final dissociation of the complex oxide occurred under more reducing conditions. The main difference between 1200 and 1000°C was the coexistence of both the perovskite phase and the transient phases of $(La,Sr)(Fe,Co)O_4$ between $10^{-16} \leq$ oxygen activity $\leq 10^{-11}$ at 1000°C. The perovskite phase disappeared at an oxygen activity of 10^{-17} (not shown in Fig. 9) which is consistent with the results on $LaFeO_3$ reported by Nakamura *et al.* (8). The $La_{0.6}Sr_{0.4}Co_{0.2}Fe_{0.8}O_3$ compositions appear to be more stable than either acceptor-doped $LaMnO_3$ or $YMnO_3$ (1, 9). The thermochemical properties of LSCF under a reducing atmosphere seem to follow the boundaries set between the two end members, $LaFeO_3$ and $LaCoO_3$. Although not shown here, the phase stability of compositions containing no Sr or Sr = 0.2 suggested that Sr content has little influence on the high-temperature phase stability (when compared to that shown for Sr = 0.4).

Measurements of dc conductivity and thermoelectricity power as a function of oxygen activity were carried out at temperatures between 1000 and 1200°C. The results are shown in Figs. 11 to 14. As shown in Figs. 11 and 12, both the conductivity and Seebeck data show

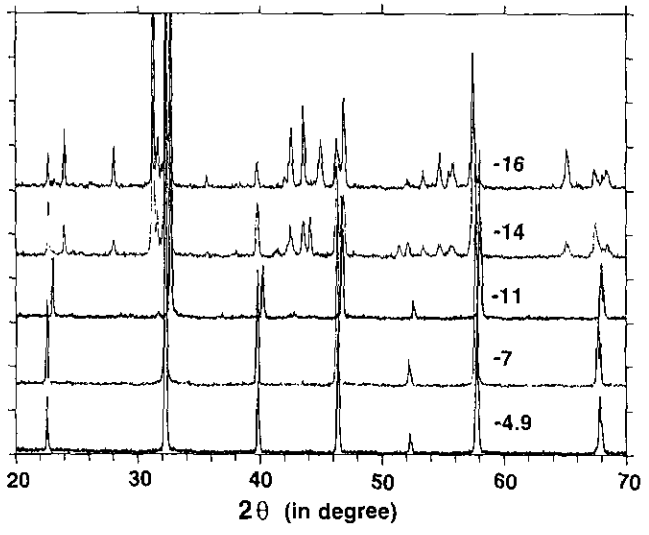

FIG. 9. XRD patterns for $La_{0.6}Sr_{0.4}Co_{0.2}Fe_{0.8}O_3$ annealed at 1000°C and quenched at given oxygen activities.

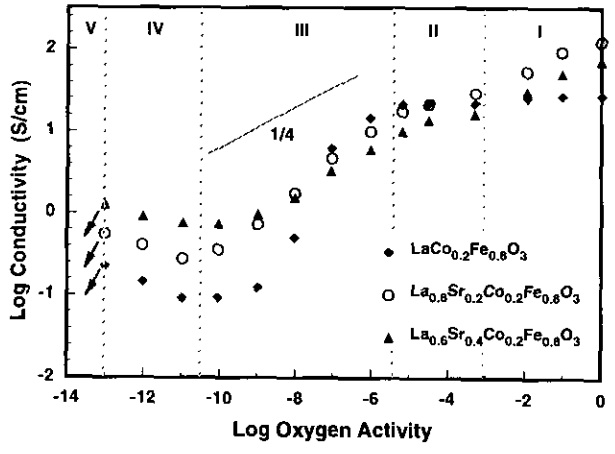

FIG. 11. Electrical conductivity of various LSCF compositions as a function of Sr content (moles) and oxygen activity equilibrated at 1200°C.

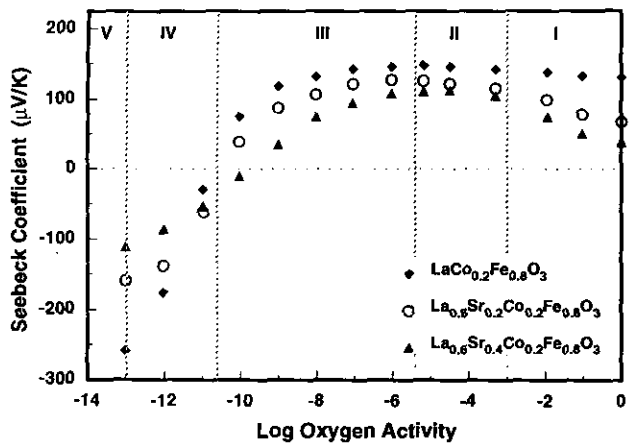

FIG. 12. Seebeck coefficient of various LSCF compositions as a function of Sr content (moles) and oxygen activity equilibrated at 1200°C.

several distinct oxygen-activity-dependent regions. In region I (oxygen activity $\geq 10^{-3}$), the decrease in electrical conductivity and increase in Seebeck coefficient indicate a switch in charge compensation from electronic to ionic. In this region both electronic and ionic compensations of the acceptor dopant are taking place with the defect reaction (according to Kröger–Vink notation) represented by (14):

$$La^{x}_{0.8}Sr'_{0.2}B^{x}_{0.8}B^{\bullet}_{0.2}O_3 \Leftrightarrow La^{x}_{0.8}Sr'_{0.2}B^{x}_{0.8+2\delta}B^{\bullet}_{0.2-2\delta}O_{3-\delta}\,[\delta V^{\bullet\bullet}_{o}] + \frac{\delta}{2}\,O_2. \quad [1]$$

Because the ionic and electronic compensations occur simultaneously and compete with each other, the electroneutrality condition can be expressed as:

$$[Sr'_{La}] = [B^{\bullet}_{B}] + 2[V^{\bullet\bullet}_{o}]. \quad [2]$$

For every oxygen vacancy (doubly ionized) formed, two p-type carriers ($B^{\bullet}_{B}$) are eliminated, which will cause an increase in the Seebeck coefficient.

The Seebeck and electrical conductivity data for all three compositions remain constant in the oxygen activity range from 10^{-3} to 10^{-5} (region II), which corresponds to the region of electronic stoichiometry (1, 11), i.e., all Co and Fe ions are at the trivalent state (or the averaged valence of all B ions is +3). This implies a reduced concentration of p-type charge carriers, as indicted by the Seebeck data shown in Fig. 12, where a maximum Seebeck coefficient is observed within this oxygen activity region. As the oxygen activity further decreases, the Seebeck coefficient starts to decrease due to the contribution of n-type conductivity to the total conductivity (region III). However, the total electrical conductivity decreases with decreasing oxygen activity. A p-to-n transition of electronic conductivity was observed when the oxygen activity reached region IV, where a conductivity minimum and zero Seebeck coefficient were observed. XRD analyses on the reduced samples indicate the presence of new phases of Co and (La,Sr)(Fe,Co)O_4 in region IV. This transition shifted to a higher oxygen activity when the Sr content was increased (see Figs. 12 and 14). When the oxide samples have multiple phases, it is not practical to interpret the electrical conductivities and/or the Seebeck data without having detailed information on the microstructure, phase identities, and oxygen contents. It is very likely that the observed p-to-n transition of electrical properties is caused by changes of the

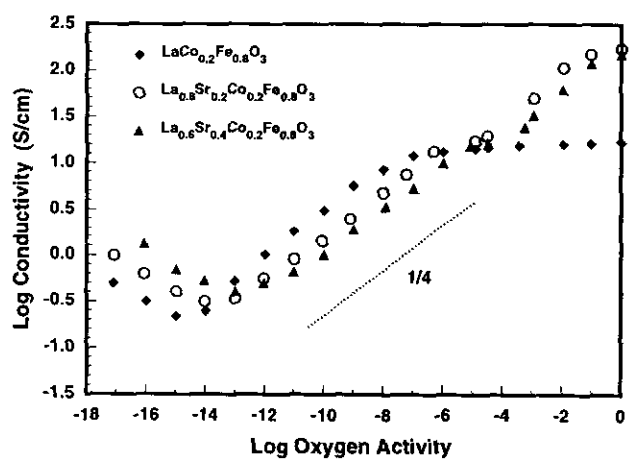

FIG. 13. Electrical conductivity of various LSCF compositions as a function of Sr content (moles) and oxygen activity equilibrated at 1000°C.

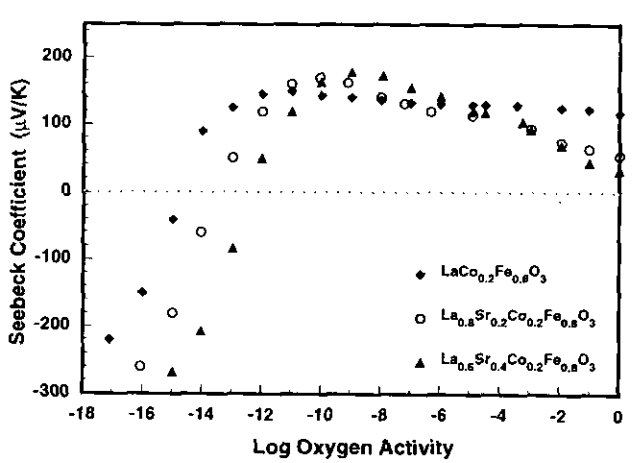

FIG. 14. Seebeck coefficient of various LSCF compositions as a function of Sr content (moles) and oxygen activity equilibrated at 1000°C.

dominating phase(s), but not simply due to the changes in charge carriers in a single oxide. In region V, the solid sample started to fully dissociate and both the electrical conductivity and thermoelectric power measurements became unstable.

A similar trend was found for samples measured at 1000°C, but the respective regions shift toward lower oxygen activity, as shown in Figs. 13 and 14. The temperature dependence of the p-to-n transition is demonstrated by Fig. 15, in which the electrical conductivity of $La_{0.6}Sr_{0.4}Co_{0.2}Fe_{0.8}O_3$ measured at three different temperatures is plotted as a function of oxygen activity. It shows that the conductivity minimum (p-to-n transition) shifts toward a higher oxygen activity as the temperature increases. As can be seen in Fig. 15, the magnitude of conductivities and the oxygen activity dependencies were almost the same over the temperature range from 1000 to 1200°C. The observed p-type conductivity in Figs. 11, 13, and 15 roughly show a positive slope of 1/4 with the oxygen activity in agreement with the defect model derived for the acceptor- (Sr'_{La}) doped $LaBO_3$ (1). Theoretically, a defect-chemistry interpretation for the observed linear dependence of electrical conductivity over oxygen activity on a log scale is only valid when the oxide is in single phase. The XRD data for various LSCF compositions, as shown in Figs. 5 through 10, imply that such a requirement is fulfilled in the above interpretation of electrical conductivity data.

The solid samples started to disintegrate at oxygen activities below 10^{-13} and 10^{-17} at 1200 and 1000°C, respectively. XRD analyses on powder samples indicate that LSCF can be reoxidized to a single-phase perovskite after total dissociation under an even more reducing atmosphere (e.g., $La_{0.6}Sr_{0.4}Co_{0.2}Fe_{0.8}O_3$ at 1200°C and an oxygen activity of 10^{-18}). Electrical conductivity measurements at oxygen activity below the dissociation oxygen activity were not possible due to the gradual degradation and eventual failure of the solid rod samples. Upon reoxidation, the electrical conductivity nearly returned to its prereduction value (within 10%). But, due to the dissociation reaction (and the consequent changes in the microstructure), a degradation of electrical conductivity was observed. The dissociation oxygen activity observed for all three compositions are plotted in Fig. 16 as function of temperature, along with the data for $LaFeO_3$ (3). Apparently, the substitution of Sr and Co for the respective La and Fe decreases the high-temperature phase stability of $LaFeO_3$, but by only about an order of magnitude.

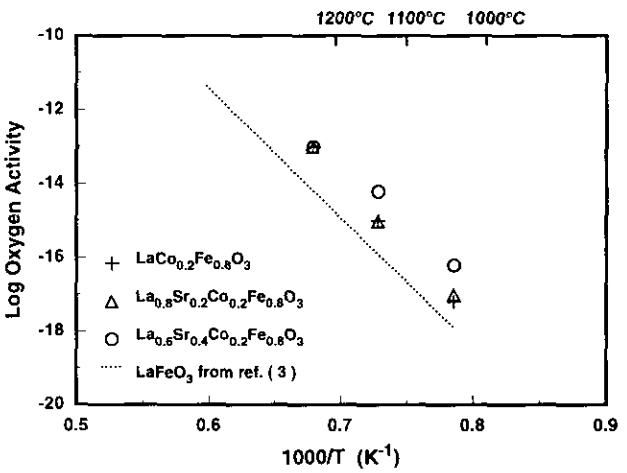

FIG. 16. The dissociation oxygen activity for various LSCF compositions and $LaFeO_3$ as a function of temperature.

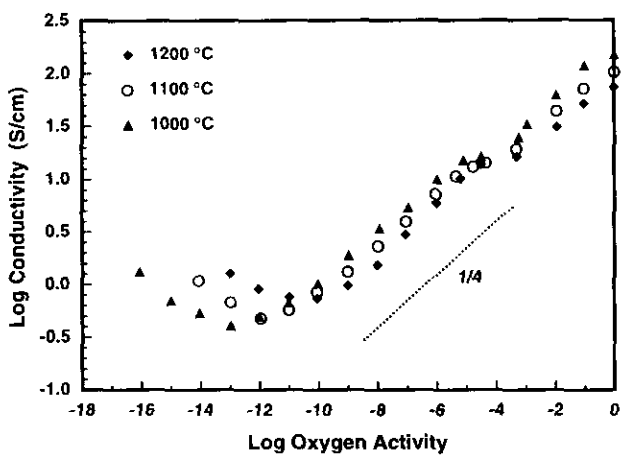

FIG. 15. Electrical conductivity of $La_{0.6}Sr_{0.4}Co_{0.2}Fe_{0.8}O_3$ as a function of oxygen activity equilibrated at different temperatures.

4. CONCLUSION

$La_{1-x}Sr_xCo_{0.2}Fe_{0.8}O_3$ (x = 0, 0.2, 0.4) compositions show a wide oxygen activity range of phase stability. Upon reduction, these oxides did not dissociate into binary oxides and metal in a simple step, but they formed transient compounds, which, with further reduction, dissociated to La_2O_3, SrO, Co, and Fe. The approximate 1/4 power dependence of the p-type electrical conductivity on the oxygen activity can be attributed to both electronic and ionic charge compensations.

ACKNOWLEDGMENTS

This research was supported by the Gas Research Institute, British Petroleum of America, and the Basic Energy Science Division of the U.S. Department of Energy.

REFERENCES

1. H. U. Anderson, *Solid State Ionics* **52**(1), 33 (1992).
2. L-W. Tai, M. M. Nasrallah, and H. U. Anderson, *in* "Proceedings, 3rd International Symposium on Solid Oxide Fuel Cells" (S. C. Singhal and H. Iwahara Eds.), p. 241 Electrochem. Soc., Pennington, NJ, 1993.
3. J. Mizusaki, T. Sasamoto, W. R. Cannon, and H. K. Bowen, *J. Am. Ceram. Soc.* **65,** 363 (1982).
4. J. Mizusaki, T. Sasamoto, W. R. Cannon, and H. K. Bowen, *J. Am. Ceram. Soc.* **66,** 247 (1983).
5. J. Mizusaki, M. Yoshihiro, S. Yamauchi, and K. Fueki, *J. Solid State Chem.* **58,** 257 (1985).
6. J. Mizusaki, Y. Mima, S. Yamauchi, K. Fueki, and H. Tagawa, *J. Solid State Chem.* **80,** 102 (1989).
7. J. Mizusaki, J. Tabuchi, T. Matsuura, S. Yamauchi, and K. Fueki, *J. Electrochem. Soc.* **136,** 7 (1989).
8. R. Nakamura, G. Petzow, L. J. and Gauckler, *Mater. Res. Bull.* **14,** 649 (1979).
9. J. H. Kuo, H. U. Anderson, and D. M. Sparlin, *J. Solid State Chem.* **83,** 52 (1989).
10. G. F. Carini II, "An Apparatus for the Measurement of dc Electrical Conductivity and Seebeck Coefficient of Semiconductors as a Function of High Temperature and Oxygen Partial Pressure," M.S. Thesis, University of Missouri–Rolla, 1987.
11. J. Mizusaki, M. Yoshihiro, S. Yamauchi, and F. Kazuo, *J. Solid State Chem.* **58,** 257 (1985).
12. J. L. Soubeyroux, L. Fourres, D. Fruchart, and G. LeFlem, *J. Solid State Chem.* **31,** 313 (1978).
13. J. J. Janecek and G. P. Wirtz, *J. Am. Ceram. Soc.* **61,** 242 (1978).
14. F. A. Kröger and H. J. Vink, "Solid State Physics," 3rd ed., Academic Press, New York, 1956.